Available online at www.sciencedirect.com
SCIENCE DIRECT®
PERGAMON
Polyhedron 22 (2003) 1857–1863
POLYHEDRON
www.elsevier.com/locate/poly

Mn_4 single-molecule magnets with a planar diamond core and $S = 9$

En-Che Yang [a], Nicholas Harden [b], Wolfgang Wernsdorfer [c], Lev Zakharov [d], Euan K. Brechin [e], Arnold L. Rheingold [d], George Christou [b,*], David N. Hendrickson [a,*]

[a] Department of Chemistry and Biochemistry, University of California at San Diego, La Jolla, CA 92093-0358, USA
[b] Department of Chemistry, University of Florida, Gainesville, FL 32611-7200, USA
[c] Laboratoire Louis Néel, CNRS BP 166, Avenue des Martyrs, 38042 Grenoble Cedex 9, France
[d] Department of Chemistry and Biochemistry, University of Delaware, Newark, DE 19716, USA
[e] Department of Chemistry, The University of Manchester, Oxford Road, Manchester M13 9PL, UK

Received 6 October 2002; accepted 14 December 2002

Abstract

The syntheses and magnetic properties are reported for three Mn_4 single-molecule magnets (SMMs): $[Mn_4(hmp)_6(NO_3)_2(MeCN)_2](ClO_4)_2 \cdot 2MeCN$ (**3**), $[Mn_4(hmp)_6(NO_3)_4] \cdot (MeCN)$ (**4**), and $[Mn_4(hmp)_4(acac)_2(MeO)_2](ClO_4)_2 \cdot 2MeOH$ (**5**). In each complex there is a planar diamond core of $Mn_2^{III}Mn_2^{II}$ ions. An analysis of the variable-temperature and variable-field magnetization data indicate that all three molecules have intramolecular ferromagnetic coupling and a $S = 9$ ground state. The presence of a frequency-dependent alternating current susceptibility signal indicates a significant energy barrier between the spin-up and spin-down states for each of these three $Mn_2^{III}Mn_2^{II}$ complexes. The fact that these complexes are SMMs has been confirmed by the observation of hysteresis in the plot of magnetization versus magnetic field measured for single crystals of complexes **3** and **4**. The hysteresis loops for both of these complexes exhibit steps characteristic of quantum tunneling of magnetization. Complex **4** shows its first step at zero field, whereas the first step for complex **3** is shifted to -0.10 T. This shift is attributable to weak intermolecular antiferromagnetic exchange interactions present for complex **3**.

Keywords: Single-molecule magnets; Nanomagnet; Magnetization tunneling; Superparamagnet; Manganese

1. Introduction

Single-molecule magnets (SMMs) have been attracting an increasing interest [1], for they provide the means to systematically study the chemistry and physics of nanomagnets. The long range goals for the research on SMMs draws from three quarters. First, a SMM may serve as the smallest single bit magnetic memory unit. Second, there is considerable interest [2] in discovering quantum effects on the mesoscopic scale in magnetism. SMMs have been shown [1,3,4] to exhibit quantum tunneling of magnetization. Third, there have been theoretical papers [5,6] to indicate that SMMs may be more than a single bit memory unit, and could be of utility in quantum computation.

In order to understand the mechanism of quantum tunneling of magnetization and how important intermolecular interactions are for SMMs it is imperative that series of related SMMs be prepared. The two most studied series of SMMs are the Mn_{12} and the $S = 9/2$ Mn_4 families. There are more than 20 structurally characterized $[Mn_{12}O_{12}(O_2CR)_{16}(H_2O)_4]$ complexes, as well as salts of singly and doubly reduced Mn_{12} complexes [7–11]. There are almost as many members in the $S = 9/2$ $Mn^{IV}Mn_3^{III}$ family [12–15].

Previously we described the preparation and properties of two Mn_4 SMMs that have integer spin ground states. Mn_4 complexes with a planar diamond core and incorporating either the monodeprotonated anions of pyridine dimethanol ($pdmH^-$) or hydroxymethylpyridine (hmp^-) with the compositions of $[Mn_4(hmp)_6Br_2(H_2O)_2]Br_2$ (complex **1**) [16,17] and $[Mn_4(pdmH)_6(OAc)_2](ClO_4)_2$ (complex **2**) [18,19] were reported. Complex **1** has a $S = 9$ ground state, whereas complex

* Corresponding authors.
E-mail addresses: christou@chem.ufl.edu (G. Christou), dhendrickson@ucsd.edu (D.N. Hendrickson).

0277-5387/03/$ - see front matter
doi:10.1016/S0277-5387(03)00173-6

2 has a $S = 8$ ground state. In the case of complex **1** the magnetization versus magnetic field plot shows a relatively small coercive field, perhaps due to intermolecular exchange interations that have been shown to be present with heat capacity and magnetic susceptibility data [16,17]. In this paper we report preliminary data for three additional Mn_4 complexes that function as SMMs.

2. Experimental

2.1. Compound preparations

All chemicals and solvents were used as received. All preparations and manipulations were performed under aerobic conditions. The complexes $[Mn_7(OH)_3(hmp)_6Cl_3]Cl\cdot(ClO_4)$ and $(NBu^n_4)[MnO_4]$ were prepared as previously described [20,21]. All the compounds 3, 4 and 5 give good agreement of elemental analysis.

2.1.1. $[Mn_4(hmp)_6(NO_3)_2(MeCN)_2](ClO_4)_2\cdot 2MeCN$ (**3**)

$Mn(ClO_4)_2\cdot 6(H_2O)$ (2.49 g, 6.9 mmol) was dissolved in 40 ml methanol, followed by addition of hmpH (1.86 g, 17 mmol). Freshly prepared solid $(NBu^n_4)[MnO_4]$ (0.625 g, 1.7 mmol) dissolved in 20 ml methanol was then added to the solution. After 2 h, sodium nitrate ($NaNO_3$, 0.35 g, 4.2 mmol) was added to the solution. A dark red–brown precipitation formed overnight. The solution was filtered and the precipitate was washed with a small amount of methanol and ethylether and then dried in air overnight. The resultant solid was then re-dissolved in acetonitrile and layered with ethylether. Red–brown crystals suitable for X-ray analysis formed after a week.

2.1.2. $[Mn_4(hmp)_6(NO_3)_4]\cdot MeCN$ (**4**)

$[Mn_7(OH)_3(hmp)_6Cl_3]Cl\cdot(ClO_4)$ (0.212 g, 0.16 mmol) was dissolved in MeCN (50 ml). To this solution 5 equiv. of $AgNO_3$ (0.094 g, 0.55 mmol) were added. The dark brown solution turned pink and an off-white precipitate formed (AgCl). The solution was filtered and a 1:2 Et_2O/hexanes mixture (100 ml) was added to afford a cerise-colored powder $[Mn_4(hmp)_6(NO_3)_4]\cdot$ MeCN.

2.1.3. $[Mn_4(hmp)_4(acac)_2(MeO)_2](ClO_4)_2\cdot 2MeOH$ (**5**)

$Mn(ClO_4)_2\cdot 6(H_2O)$ (3.6 g, 10 mmol) and hmpH (1.1 g, 10 mmol) was dissolved in 30 ml methanol followed by addition of a solution of acac (1 g, 10 mmol) and sodium methoxide (0.54 g, 10 mmol) in 30 ml methanol. After 2 h, the solution was filtered and layered with ethylether. Dark brown crystals formed after 1–2 weeks.

2.2. Physical measurements

Alternating current (ac) magnetic susceptibility measurements were made with a MPMS2 Quantum Design SQUID magnetometer equipped with an 1T magnet and capable of achieving temperatures of 1.7–400 K. The a.c. field range is 1×10^{-4} to 5 G, oscillating in a frequency range of 5×10^{-4}–1512 Hz. Pascal's constants [22] were used to approximate the diamagnetic molar susceptibility contribution for each complex that were subtracted from the experimental molar susceptibility data to give the molar paramagnetic susceptibility data. Ac magnetic susceptibility data were collected on microcrystalline and frozen solution samples in an a.c. field of 1 G and a dc field of 0 G. Variable-temperature and variable-field magnetization data were collected on a Quantum Design MPMS5 SQUID magnetometer. Samples were restrained in eicosane by first keeping the samples at a temperature above the melting point (308–310 K) of eicosane for 15 min, then the temperature was gradually decreased below the melting point to solidify the eicosane in order to restrain the crystals. Magnetization versus magnetic field hysteresis data were determined for complexes **3** and **4** by means of the micro-SQUID technique that is described elsewhere [23].

3. Results and discussion

3.1. Structures

ORTEP plots of the $[Mn_4(hmp)_6(NO_3)_2(MeCN)_2]^{2+}$ cation in complex **3**, the complex **4** $[Mn_4(hmp)_6(NO_3)_4]$ and the $[Mn_4(hmp)_4(acac)_2(MeO)_2]^{2+}$ cation in complex

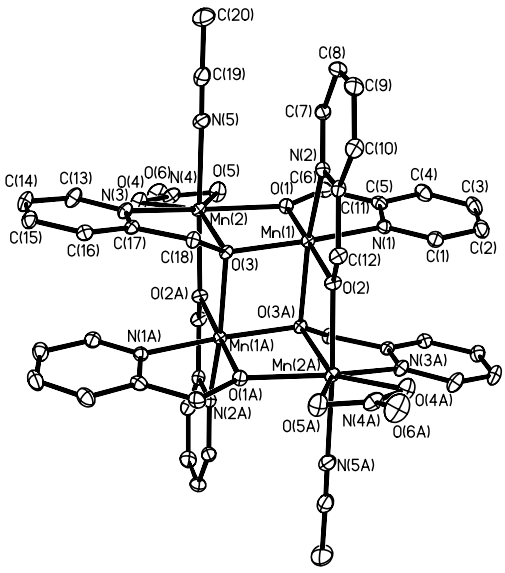

Fig. 1. ORTEP representation of the $[Mn_4(hmp)_6(NO_3)_2(MeCN)_2]^{2+}$ cation in complex **3** showing 50% probability ellipsoids.

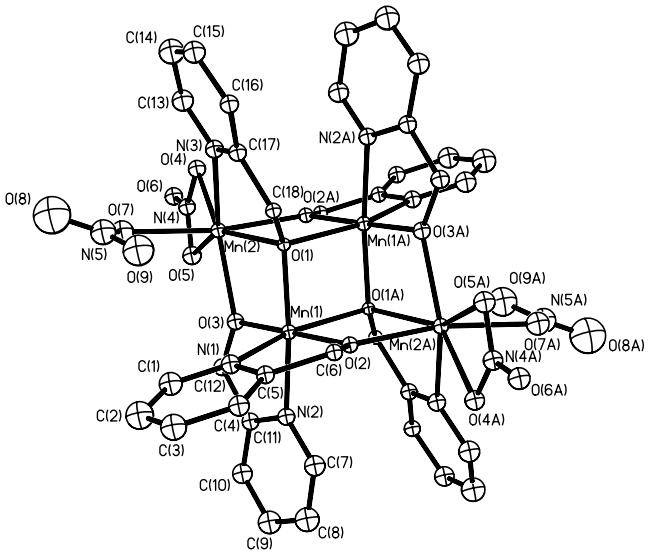

Fig. 2. ORTEP representation of complex **4** showing 30% probability ellipsoids.

5 are shown in Figs. 1–3. All three complexes are mixed-valence, consisting of $2Mn^{II}$ and $2Mn^{III}$ ions and have a planar diamond core. In complexes **3** and **4**, the monoanionic bidentate 2-hydroxymethylpyridine anion (hmp^-) serves as the only bridging ligand, whereas in complex **5** oxygen atoms of both hmp^- and MeO^- serve as the bridging ligands. The Mn_4 'dicubanes' in all three complexes are composed of two Mn_3 triangular faces held together by an μ_3-oxygen atom from the hmp^- (complexes **3** and **4**) and MeO^- (complex **5**). The manganese ions on the common edge of the two triangular faces are six coordinate and assigned to Mn^{III} ions on the basis of the presence of a Jahn–Teller elongation. The other two Mn ions (not on the common edge of the two triangular faces) are assigned as Mn^{II} ions that are seven coordinate in complexes **3** and **4**, and six coordinate in complex **5**.

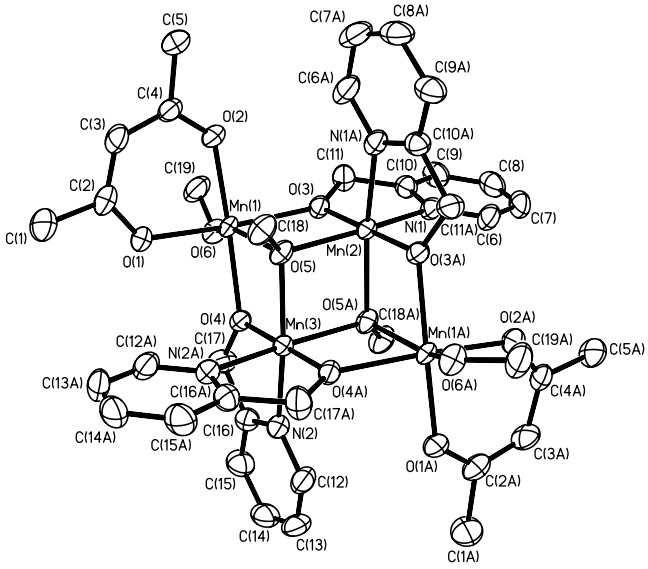

Fig. 3. ORTEP representation of the $[Mn_4(hmp)_4(acac)_2(MeO)_2]^{2+}$ cation in complex **5** showing 50% probability ellipsoids.

3.2. DC magnetic susceptibility

The $\chi_M T$ versus temperature data for these three complexes were fit in order to determine the exchange parameters characterizing the magnetic exchange interactions in complexes **3**–**5**. The experimental data were least-squares fit employing the Kambe approach where only two dominant exchange pathways are considered (Fig. 4). The spin Hamiltonian is given in Eq. (1).

$$\hat{H} = -J_{wb}(\hat{S}_T^2 - 2\hat{S}_A^2 - \hat{S}_B^2) - J_{bb}(\hat{S}_A^2 - \hat{S}_1^2 - \hat{S}_3^2) \quad (1)$$

where

$$\hat{S}_A = \hat{S}_1 + \hat{S}_3, \quad \hat{S}_B = \hat{S}_2 + \hat{S}_4, \quad \text{and} \quad \hat{S}_T = \hat{S}_A + \hat{S}_B \quad (2)$$

The Kambe equivalent operator approach gives the eigenvalue expression in Eq. (3).

$$E(S_T) = -J_{wb}[S_T(S_T+1) - S_A(S_A+1) - S_B(S_B+1)] - J_{bb}[S_A(S_A+1)] \quad (3)$$

With two $S = 2$ and two $S = 5/2$ interacting ions there are a total of 110 possible states with S_T, the total spin of the Mn_4 cluster, ranging from 0 to 9. The experimental data obtained under 1 Tesla for all three molecules shows a $\chi_M T$ value of approximately 15–16 (cm^3 K mol^{-1}) at 300 K and this increases to 32 (cm^3 K mol^{-1}) at 15 K, then decreases abruptly upon decreasing the temperature. The data below 15 K were omitted in the fitting, because zero-field and magnetization saturation effects are likely to influence the data in this temperature range. The results of fitting the experimental data are shown as solid lines in Figs. 5–7. The final fitting parameters are $g = 1.87$, $J_{bb} = 9.9$ cm^{-1}, $J_{wb} = 1.0$ cm^{-1} for complex **3**; $g = 1.99$, $J_{bb} = 6.3$ cm^{-1}, $J_{wb} = 4.2$ cm^{-1} for complex **4**; $g = 1.93$, $J_{bb} = 5.3$ cm^{-1}, $J_{wb} = 0.78$ cm^{-1} for complex **5**. It is clear that all three molecules are ferromagnetically coupled to give a $S = 9$ ground state.

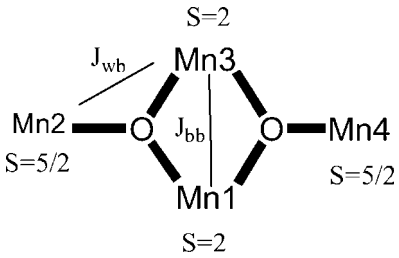

Fig. 4. Diagram showing the definition of atom number and magnetic exchange parameters for the three Mn_4 complexes studied.

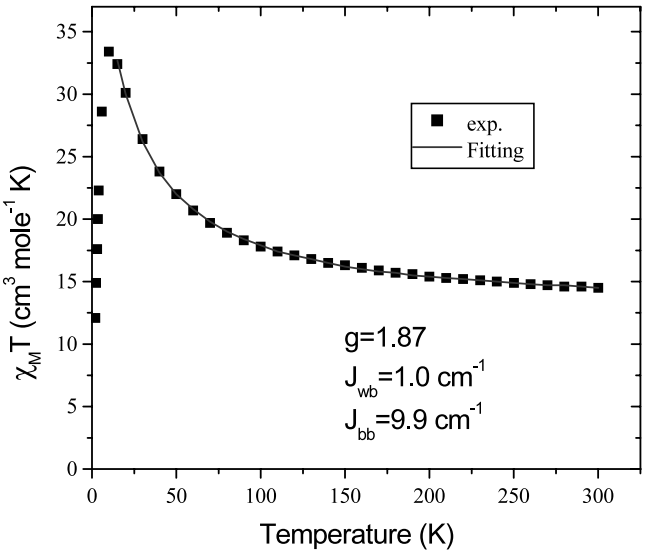

Fig. 5. Plot of $\chi_M T$ versus temperature for a powdered sample of complex **3**, where χ_M is the molar paramagnetic susceptibility. The solid line represents a least-squares fit of the data in the 15–300 K region.

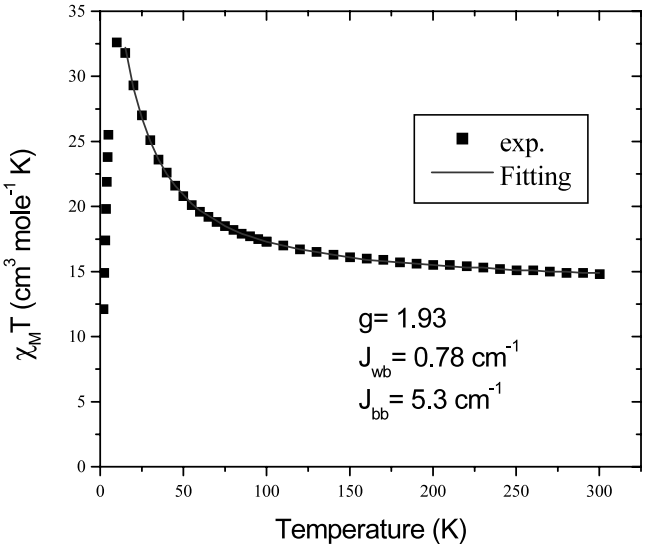

Fig. 7. Plot of $\chi_M T$ versus temperature for a powder sample of complex **5**, where χ_M is the molar paramagnetic susceptibility. The solid line represents a least-squares fit of the data in the 15–300 K region.

3.3. Variable-field DC magnetization

In order to further characterize the ground state spin S, and the g and zero-field splitting D values for the ground state, complexes **3**–**5** were further examined by variable-field dc magnetization measurements with applied magnetic fields of 10–50 kG in the 2–4 K range. In this measurement, the reduced magnetization $M/(N\mu_B)$ versus H/T is calculated, where M is the magnetization, N is Avogadro's number, μ_B is the Bohr magneton, and H is the magnetic field. The resultant reduced magnetization fitting (full matrix diagonalization with a powder average) gives the spin parameters as $S = 9$, $g = 1.84$ and $D/k_B = -0.27$ K for complex **3**; $S = 9$, $g = 1.84$ and $D/k_B = -0.31$ K for complex **4**; and $S = 9$, $g = 2.04$ and $D/k_B = -0.31$ K for complex **5**.

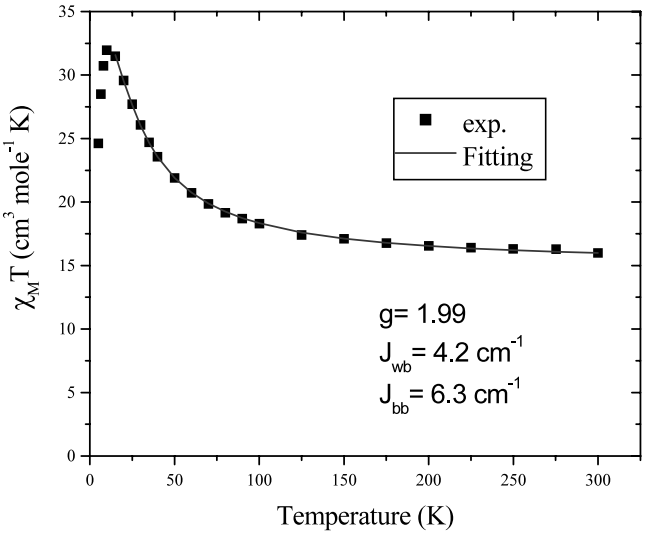

Fig. 6. Plot of $\chi_M T$ versus temperature for a powder sample of complex **4**, where χ_M is the molar paramagnetic susceptibility. The solid line represents a least-squares fit of the data in the 15–300 K region.

3.4. AC magnetic susceptibility

Evidence that complexes **3**–**5** function as SMMs was obtained with a.c. magnetic susceptibility measurements. In order for a molecule to be a SMM, it must possess both a large spin ground state and negative magnetoanisotropy to give rise to an energy barrier between the spin-up and spin-down states. Therefore, if an oscillating magnetic field is applied at low temperatures, a reduction in the in-phase (χ'_M) signal and a corresponding increase in the out-of-phase (χ''_M) signal are seen. The sluggish relaxation of magnetization is due to the energy barrier. Powdered polycrystalline samples of **3**–**5** were studied in the 1.8–10 K range with a 1 G a.c. field oscillating in the range of 50–1000 Hz (50–1500 Hz for complex **4**), see Figs. 8–10. At temperatures below 3 K there are significant increases of the out-of-phase signal accompanied by collapses of the in-phase signal. The frequency dependence of the a.c. signals suggests that all three complexes are SMMs.

3.5. Magnetization hysteresis data

The fact that complexes **3** and **4** are SMMs has been further confirmed by magnetization versus magnetic field hysteresis measurements, the results of which are shown in Figs. 11 and 12. The hysteresis loops were taken in a temperature range 0.04–1.2 K for complex **3**

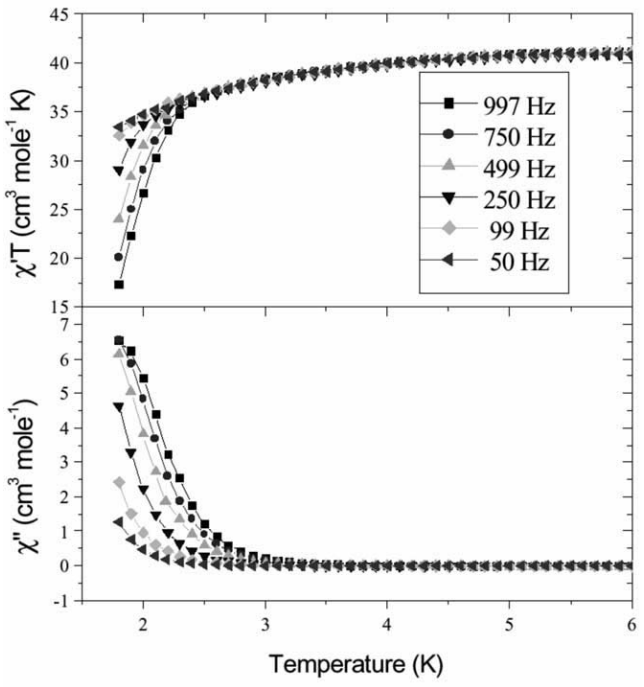

Fig. 8. Plot of $\chi'_{M}T$ (top) and χ''_{M} (bottom) versus temperature for a polycrystalline sample of complex **3** in a 1.0 G a.c. field.

and 0.04–1.05 K for complex **4** with a scanning rate of 0.07 T s^{-1} for complex **3** and **4**. The samples were first saturated in a field of −1 T and swept down to 1 T, and then cycled back to −1 T. Steps are seen at regular intervals of external field for both complexes **3** and **4**. Clearly, complexes **3** and **4** exhibit resonant quantum tunneling of magnetization. The coercive fields observed

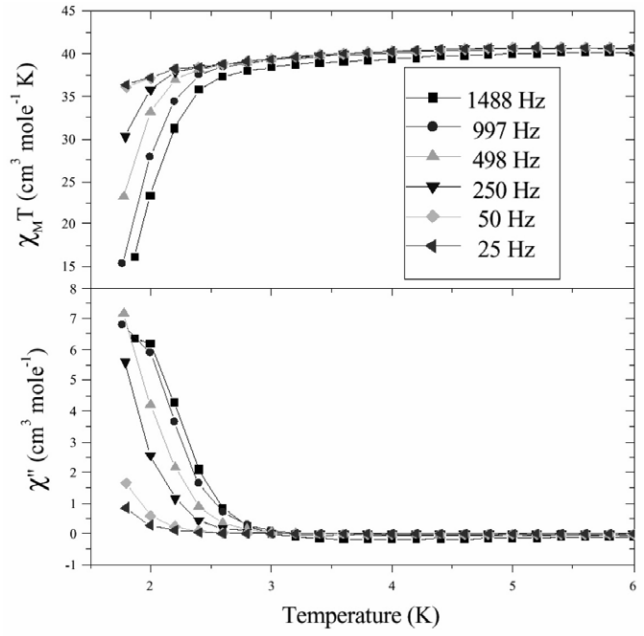

Fig. 9. Plot of $\chi'_{M}T$ (top) and χ''_{M} (bottom) versus temperature for a polycrystalline sample of complex **4** in a 1.0 G a.c. field.

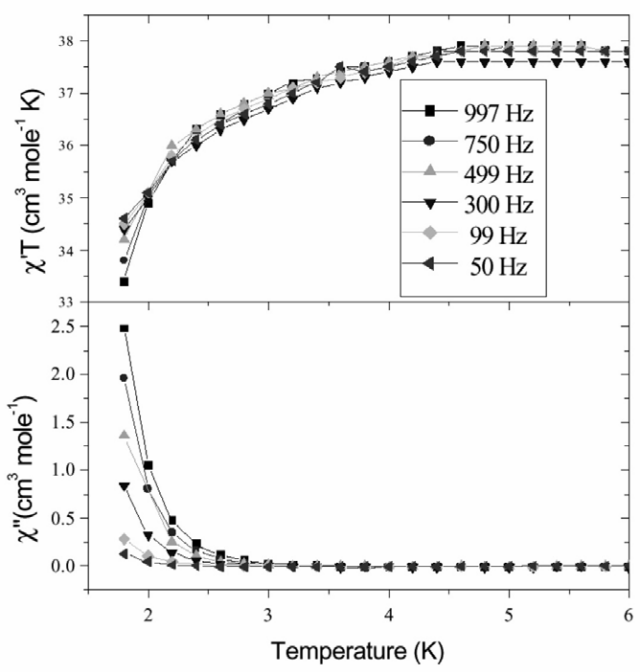

Fig. 10. Plot of $\chi'_{M}T$ (top) and χ''_{M} (bottom) versus temperature for a polycrystalline sample of complex **5** in a 1.0 G a.c. field.

for both complexes are appreciable. This is in contrast to the smaller coercive field observed [16,17] for Mn_4 complex **1**. It has been shown that there are significant intermolecular magnetic exchange interactions present for complex **1**. There are both intermolecular Br···Br contacts and π–π interactions of pyridine moieties in complex **1** and these must lead to the reduced coercive field observed. Thus, complex **1** has a greater rate of quantum tunneling due to larger transverse interactions and/or spin–spin cross relaxation [15].

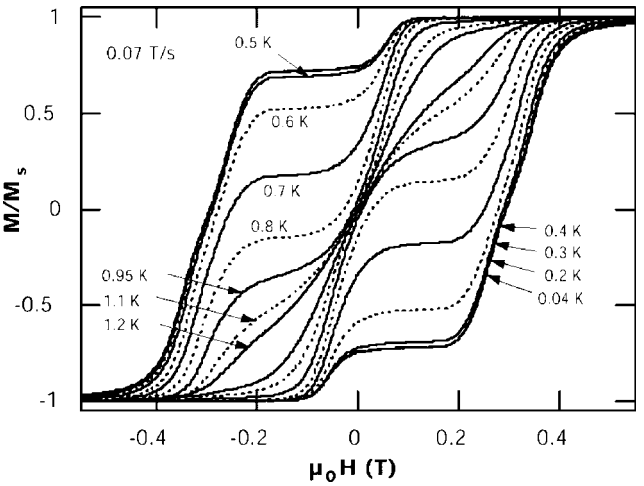

Fig. 11. Plot of hysteresis loop for complex **3** with scanning rate 0.07 T s^{-1} in the temperature range of 0.04–1.2 K. The hysteresis loop are temperature independent below 0.4 K indicating quantum tunneling on the ground state.

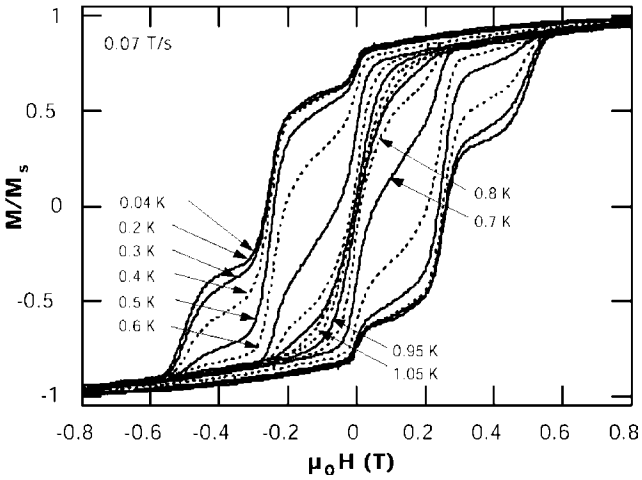

Fig. 12. Plot of hysteresis loop for complex **4** with scanning rate 0.14 T s^{-1} in the temperature range of 0.04–1.05 K. The hysteresis loop are temperature independent below 0.25 K indicating ground state quantum tunneling.

A very interesting observation can be made by comparing the magnetization loops shown in Figs. 11 and 12 for complexes **3** and **4**, respectively. The first step for magnetization tunneling is seen at zero field for complex **4**, whereas the first step for complex **3** is shifted to −0.1 T. There is an 'exchange bias' in the magnetic field at which magnetization tunneling occurs for complex **3**. In a very recent paper [24], it was shown that an antiferromagnetic exchange interaction between two $S = 9/2$ Mn_4 SMMs in a $[Mn_4]_2$ dimer led to a −0.33 T exchange bias in the magnetization tunneling. Six hydrogen bonding contacts together with a Cl···Cl contact within the $[Mn_4]_2$ dimer gave a weak ($J = -0.05$ K for $-2J\hat{S}_1 \cdot \hat{S}_2$) antiferromagnetic exchange interaction. Thus, the exchange interaction shifts the magnetic field at which an avoided crossing of two energy levels occurs and the first step in the hysteresis loop is shifted to −0.33 T. It must be emphasized that the antiferromagnetic interaction in this case is between only two $S = 9/2$ molecules. However, even more recently we showed [25] that an exchange interaction that extends three dimensionally throughout the lattice also produces significant exchange biasing of the field at which magnetization tunneling occurs. Cl···Cl contacts between neighboring $S = 4$ Ni_4 SMM moleucles that develop throughout the lattice led in one case to a shift from zero-field to −0.7 T for the first tunneling step.

It has to be concluded that the Mn_4 complex **3** must possess intermolecular exchange interactions that cause the −0.1 T shift, see Fig. 11. Indeed, examination of the crystal packing for complex **3** shows that there is a π–π interaction likely between the hmp^- pyridine units on neighboring Mn_4 complexes, see Fig. 13. Although the two pyridine units are not eclipsing each other, this interaction occurs between pairs of Mn_4 complexes in an extended fashion. This could be sufficient to cause the

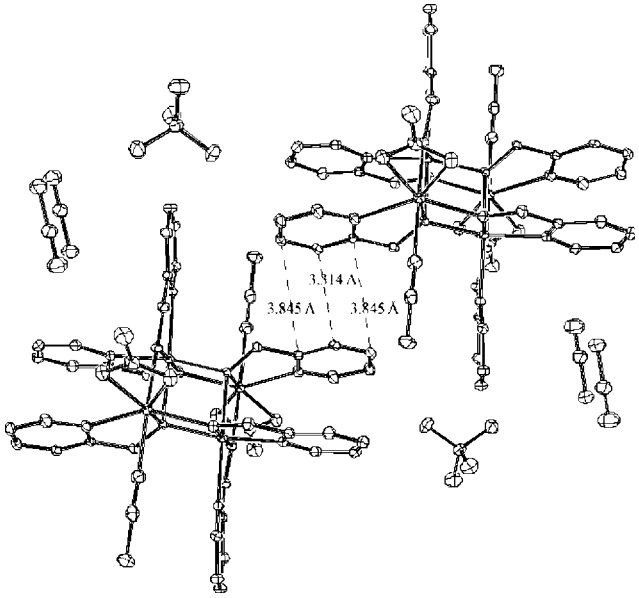

Fig. 13. Packing diagram of complex **3** in crystal lattice showing the intermolecular π–π interaction between two $[Mn_4(hmp)_6(NO_3)_2(MeCN)_2]^{2+}$ cations. An overlap between two pyridine moieties is present.

relatively small exchange bias of −0.1 T that is observed. Insulating substituents could be added to the hmp^- pyridine moiety to eliminate this intermolecular interaction and this should remove the exchange bias.

4. Conclusions

Three $Mn^{III}_2Mn^{II}_2$ complexes have been synthesized and characterized. The magnetic properties of metal complexes **3**–**5** have been studied and all three complexes have a $S = 9$ ground state with $D < 0$. A frequency dependence of the out-of-phase a.c. magnetic susceptibility signal indicates that complexes **3** and **4** are SMMs. Well developed magnetization hysteresis loops with appreciable coercive fields are seen for both complexes. Interestingly, complex **3** exhibits a −0.1 T exchange bias, ie, a shift in the first step in the hysteresis loop.

5. Supplementary material

Crystallographic data for the structural analysis have been deposited with the Cambridge Crystallographic Data Centre, CCDC No. 195523, 195524 and 195525. Copies of this information may be obtained free of charge from the Director, CCDC, 12 Union Road, Cambridge, CCB2 1EZ, UK (fax: +44-1223-336033; e-mail: deposit@ccdc.cam.ac.uk or www: http://www.ccdc.cam.ac.uk).

Acknowledgements

This work was supported by the National Science Foundation.

References

[1] G. Christou, D. Gatteschi, D.N. Hendrickson, R. Sessoli, MRS Bull. 25 (2000) 66.
[2] I. Tupitsyn, B. Barbara, in: J.S. Miller, M. Drillon (Eds.), Magnetism: Molecules to Materials III, chapter 4), Wiley-VCH, Weinheim, Germany, 2002, pp. 109–168.
[3] (a) J.R. Friedman, M.P. Sarachik, J. Tejada, J. Maciejewski, R. Ziolo, J. Appl. Phys. 79 (1996) 6031;
(b) J.R. Friedman, M.P. Sarachik, J. Tejada, R. Ziolo, Phys. Rev. Lett. 76 (1996) 3830.
[4] L. Thomas, F. Lionti, F.R. Ballou, D. Gatteschi, R. Sessoli, B. Barbara, Nature 383 (1996) 145.
[5] M.N. Leuenberger, D. Loss, Nature 410 (2001) 789.
[6] B. Zhou, R. Tao, S. Shen, J. Liang, Phys. Rev. A 66 (1) (2002) 010301.
[7] H.J. Eppley, H.-L. Tsai, N. de Vries, K. Folting, G. Christou, D.N. Hendrickson, J. Am. Chem. Soc. 117 (1995) 301.
[8] S.M.J. Aubin, S. Spagna, H.J. Eppley, R.E. Sager, G. Christou, D.N. Hendrickson, J. Chem. Soc., Chem. Commun. (1998) 803.
[9] S.M.J. Aubin, Z. Sun, L. Pardi, J. Krzystek, K. Folting, L. Brunel, A.L. Rheingold, G. Christou, D.N. Hendrickson, Inorg. Chem. 38 (1999) 5329.
[10] M. Soler, S.K. Chandra, D. Ruiz, E.R. Davidson, D.N. Hendrickson, G. Christou, J. Chem. Soc., Chem. Commun. (2000) 2417.
[11] T. Kuroda-Sowa, M. Lam, A.L. Rheingold, C. Frommen, W.M. Reiff, M. Nakano, J. Yoo, A.L. Maniero, L.-C. Brunel, G. Christou, D.N. Hendrickson, Inorg. Chem. 40 (2001) 6469.
[12] S. Wang, H.-L. Tsai, E. Libby, K. Folting, W.E. Streib, D.N. Hendrickson, G. Christou, Inorg. Chem. 35 (1996) 7578.
[13] S.M.J. Aubin, N.R. Dilley, M.W. Wemple, M.B. Maple, G. Christou, D.N. Hendrickson, J. Am. Chem. Soc. 120 (1998) 839.
[14] H. Andres, R. Basler, H.-U. Gudel, G. Aromi, G. Christou, H. Buttner, B. Ruffle, J. Am. Chem. Soc. 122 (2000) 12469.
[15] W. Wernsdorfer, S. Bhaduri, R. Tiron, D.N. Hendrickson, G. Christou, Phys. Rev. Lett. 89 (2002) 197201.
[16] J. Yoo, A. Yamaguchi, M. Nakano, J. Krzystek, W.E. Streib, L.-C. Brunel, H. Ishimoto, G. Christou, D.N. Hendrickson, Inorg. Chem. 40 (2001) 4604.
[17] A. Yamaguchi, N. Kusumi, H. Ishimoto, H. Mitamura, T. Goto, N. Mori, M. Nakano, K. Awaga, J. Yoo, D.N. Hendrickson, G. Christou, J. Phys. Soc. Jpn 71 (2002) 414.
[18] E.K. Brechin, J. Yoo, M. Nakano, J.C. Huffman, D.N. Hendrickson, G. Christou, J. Chem. Soc., Chem. Commun. (1999) 783.
[19] J. Yoo, E.K. Brechin, A. Yamaguchi, M. Nakano, J.C. Huffman, A.L. Maniero, L. Brunel, K. Awaga, H. Ishimoto, G. Christou, D.N. Hendrickson, Inorg. Chem. 39 (2000) 3615.
[20] M.A. Bolcar, S.M.J. Aubin, K. Folting, D.N. Hendrickson, G. Christou, J. Chem. Soc., Chem. Commun. (1997) 1485.
[21] T. Sala, M.V. Sargent, J. Chem. Soc., Chem. Commun. (1978) 253.
[22] E.A. Boudreaux, in: E.A. Boudreaux, L.N. Mulay (Eds.), Theory and Applications of Molecular Paramagnetism, Wiley, New York, 1976.
[23] W. Wernsdorfer, Adv. Chem. Phys. 118 (2001) 99.
[24] W. Wernsdorfer, N. Aliaga-Alcade, D.N. Hendrickson, G. Christou, Nature 416 (2002) 406.
[25] E.-C. Yang, W. Wernsdorfer, S.O. Hill, R.S. Edwards, M. Nakano, S. Maccagnano, L.N. Zakharov, A.L. Rheingold, G. Christou, D.N. Hendrickson, Polyhedron 22 (2003) X-ref: 10.1016/S02775387(03)001499.